J. Am. Soc. Mass Spectrom. (2016) 27:1156–1164
DOI: 10.1007/s13361-016-1389-x

RESEARCH ARTICLE

Probing the Time Scale of FPOP (Fast Photochemical Oxidation of Proteins): Radical Reactions Extend Over Tens of Milliseconds

Siavash Vahidi, Lars Konermann

Department of Chemistry, The University of Western Ontario, London, Ontario N6A 5B7, Canada

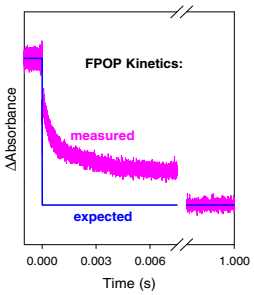

Abstract. Hydroxyl radical (·OH) labeling with mass spectrometry detection reports on protein conformations and interactions. Fast photochemical oxidation of proteins (FPOP) involves ·OH production via H_2O_2 photolysis by UV laser pulses inside a flow tube. The experiments are conducted in the presence of a scavenger (usually glutamine) that shortens the ·OH lifetime. The literature claims that FPOP takes place within 1 μs. This ultrafast time scale implies that FPOP should be immune to labeling-induced artifacts that may be encountered with other techniques. Surprisingly, the FPOP time scale has never been validated in direct kinetic measurements. Here we employ flash photolysis for probing oxidation processes under typical FPOP conditions. Bleaching of the reporter dye cyanine-5 (Cy5) served as readout of the time-dependent radical milieu. Surprisingly, Cy5 oxidation extends over tens of milliseconds. This time range is four orders of magnitude longer than expected from the FPOP literature. We demonstrate that the glutamine scavenger generates metastable secondary radicals in the FPOP solution, and that these radicals lengthen the time frame of Cy5 oxidation. Cy5 and similar dyes are widely used for monitoring the radical dose experienced by proteins in solution. The measured Cy5 kinetics thus strongly suggest that protein oxidation in FPOP extends over a much longer time window than previously thought (i.e., many milliseconds instead of one microsecond). The optical approach developed here should be suitable for assessing the performance of future FPOP-like techniques with improved temporal labeling characteristics.

Keywords: Protein structure, Oxidative labeling, Flash photolysis, Dye bleaching, Radical chemistry

Received: 13 February 2016/Revised: 9 March 2016/Accepted: 14 March 2016/Published Online: 11 April 2016

Introduction

Mass spectrometry (MS) has become indispensable for structural biology [1]. Native electrospray ionization (ESI)-MS and ion mobility spectrometry yield information on quaternary structure and subunit connectivities [2–4]. Hydrogen/deuterium exchange reports on secondary structure and dynamics [5–8]. Cross-linking provides distance constraints that can be essential for structure determination efforts [9–13].

Covalent labeling represents another important approach for monitoring protein conformations and interactions [14–19]. Solvent-accessible side chains can be modified by water-soluble reactive species, whereas buried segments are sterically protected. Numerous covalent labeling agents have been developed [14]. The resulting modification patterns can be probed by peptide mapping, liquid chromatography, and ESI-MS/MS. A potential problem associated with covalent labeling is the fact that side chain modifications can alter protein structures. Thus, if a sample is exposed to prolonged labeling the modification pattern may reflect a distorted structure, rather than the conformation of interest. This issue can be addressed by using low labeling levels, but such conditions cause analytical challenges because modification sites will have limited abundance. Kinetic tests, although cumbersome, can help identify a regime where labeling-induced structural distortion is negligible [14].

Hydroxyl radical (·OH) is one of the most widely utilized covalent labeling probes. Its small size, high reactivity, and water-like properties makes it an excellent reagent for tagging solvent-accessible surface areas. ·OH can be produced by Fenton chemistry [20, 21], electrochemical methods [22],

Electronic supplementary material The online version of this article (doi:10.1007/s13361-016-1389-x) contains supplementary material, which is available to authorized users.

Correspondence to: Lars Konermann; *e-mail:* konerman@uwo.ca

corona discharge techniques [23], water radiolysis [24–26], and photochemical cleavage of H_2O_2 [27–29]. All 20 amino acids can react with ·OH; about half of them generate products (often +16 Da modifications) that are readily detectable by MS [25].

Hambly and Gross [30] were the first to conduct protein oxidative labeling in a flow system with ·OH production via H_2O_2 photolysis by ultraviolet laser pulses. The acronym FPOP (fast photochemical oxidation of proteins) has been coined for this technique [31]. It was claimed that FPOP goes to completion within ~1 μs. This extraordinarily short time frame has important implications. First, under single-hit conditions, FPOP should be immune to labeling-induced artifacts because protein tagging will be complete *before* conformational changes can take place [30–32]. Secondly, FPOP holds promise for examining short-lived protein folding intermediates [33]. FPOP has been adopted by various researchers, and it has been applied to a range of protein systems [34–45].

Surprisingly, the time scale of oxidative labeling during FPOP has never been verified experimentally. Instead, the assertion of a ~1 μs labeling pulse is based on kinetic estimates [30], indirect statistical data [31], and stationary (not time-resolved) dosimetry [32]. It is instructive to revisit the key arguments [30]. Photochemical cleavage of hydrogen peroxide by a nanosecond laser pulse generates radicals according to $H_2O_2 \rightarrow 2$ ·OH. In purely aqueous solution and for an initial ·OH concentration of 1 mM [32], the recombination (2 ·OH → H_2O_2, $k = 6 \times 10^9$ M^{-1} s^{-1}) [46] will follow the profile of Figure 1a, where a significant ·OH concentration persists over a few μs and beyond. FPOP employs scavengers (usually Gln) to shorten the ·OH lifetime. Gln has a rate constant of 5.4×10^8 M^{-1} s^{-1} for reaction with ·OH [25]. The ·OH concentration profile calculated under pseudo-first order conditions for [Gln] = 20 mM drops close to zero within 1 μs (blue line, Figure 1b) [30]. This plot represents the foundation of the claim that FPOP is a microsecond covalent labeling technique [30–32].

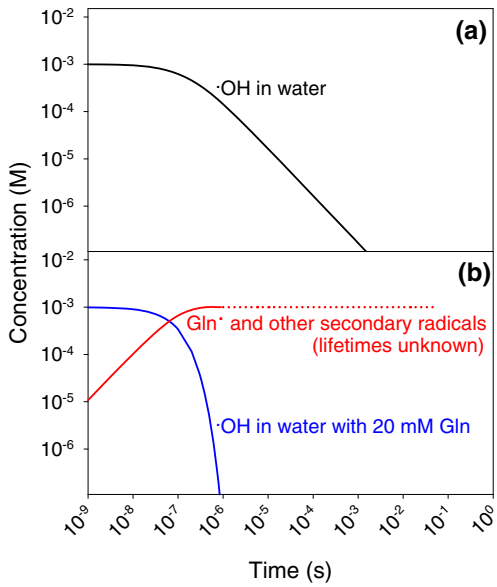

Figure 1. Calculated radical concentrations during FPOP under different conditions. **(a)** Aqueous solution containing ·OH as only solute. ·OH depletion due to radical recombination is given by $[\cdot OH] = [\cdot OH]_0/(1+kt[\cdot OH]_0)$. **(b)** Aqueous solution containing ·OH and 20 mM scavenger (Gln). Blue profile: ·OH depletion caused by reaction with Gln, $[\cdot OH] = [\cdot OH]_0 \exp(-kt[Gln]_0)$. Parameters are from reference [30]. Red profile in **(b)**: formation of secondary radicals, assuming a 1:1 molar ratio relative to the depletion of ·OH

We do not dispute that the ·OH concentration in FPOP drops to negligible values within ~1 μs. However, a comprehensive discussion has to include *all* reactive species in the solution. Most oxygen atoms incorporated into side chains during FPOP do not originate directly from ·OH (addition to aromatic residues is a possible exception) [25]. More commonly, ·OH abstracts a hydrogen, and the resulting radical undergoes a series of reactions involving dissolved O_2, culminating in +16 Da (or other) products [25, 47]. Importantly, hydrogen abstraction and subsequent oxidation can also be triggered by radicals *other than* ·OH [46–48]. Hence, one has to ask if "secondary radicals" may be formed under FPOP conditions, and whether such species can cause protein labeling after ·OH has disappeared.

The FPOP literature implicitly assumes that labeling is terminated once ·OH has interacted with the Gln scavenger. However, reaction of an odd-numbered electron species (·OH) with an even-numbered electron species (the scavenger) necessarily generates a new radical. Thus, the scavenger will generate secondary radicals according to [25, 46, 47, 49]

$$\cdot OH + Gln \rightarrow H_2O + Gln\cdot \quad (1)$$

Formation of $HO_2\cdot$ (from the reaction of ·OH with H_2O_2) can take place as well [47], followed by Haber-Weiss chain reactions that may produce additional reactive species [25]. Other secondary radicals form when Gln· reacts with dissolved O_2 close to the diffusion limit [47, 49], thereby generating peroxyl species [25, 46, 47, 49]

$$Gln\cdot + O_2 \rightarrow Gln\text{-}O\text{-}O\cdot \quad (2)$$

Transformations involving peroxyl radicals are not as fast as direct ·OH-mediated processes, e.g., reactions with methionine take place with rate constants of ~10^6 M^{-1} s^{-1} versus ~10^9 M^{-1} s^{-1} [25, 50]. Nonetheless, the cumulative oxidation caused by these secondary radicals in biological samples can be significant because of their long lifetimes [47, 51].

The formation of secondary radicals is schematically indicated by the red profile in Figure 1b. Owing to their complex chemistry, it is difficult to predict how long these species will persist in the FPOP solution [47, 49]. It cannot be ruled out that secondary radicals contribute to analyte oxidation within the FPOP flow tube. In other words, the claim that FPOP labeling is restricted to a ~1 μs time scale [30–32] has to be carefully re-examined.

Here we use flash photolysis to probe the time scale of FPOP. Direct measurements of side chain oxidation kinetics are difficult. We therefore record spectral changes of a reporter

dye in the FPOP solution. The premise of these experiments is that oxidation will alter the spectroscopic properties of the reporter dye. This approach is closely related to the widespread use of dyes as dosimeter molecules in protein samples [21, 25, 52]. We uncover major discrepancies between expected and actual oxidation kinetics. Reporter dye oxidation extends over a time period that is four orders of magnitude longer than expected.

Experimental

Reagents

Horse holo-myoglobin, Gln, Met, Arg, and organic dyes were purchased from Sigma (St. Louis, MO, USA). Apo-myoglobin (apo-Mb) was prepared as described [35]. All aqueous protein samples contained 10 mM sodium phosphate buffer at pH 7, unless noted otherwise. For some experiments, the solutions were acidified to pH 2 by addition of HCl.

Oxidative Labeling

FPOP experiments on apo-Mb were conducted using a continuous-flow device as described [35]. A two-syringe mixing approach was used to suppress background oxidation by only exposing the protein (from syringe 1) to H_2O_2 (from syringe 2) immediately prior to laser irradiation. The contents of both syringes were mixed on-line and pumped through a fused silica labeling capillary (TSP100170 Polymicro Technologies, Phoenix, AZ, USA, inner diameter 100 μm) at a total flow rate of 40 μL min^{-1}, corresponding to an average flow velocity within the capillary of 84.5 mm s^{-1}. The final mixture contained 0.1% H_2O_2, 20 mM Gln, and 10 μM protein at pH 7 or pH 2. A GAM EX50 excimer laser (Orlando, FL, USA) generating 18 ns laser pulses at 64 Hz, 248 nm, and 37.5 mJ was used for · OH production 40 cm downstream of the mixer. These experimental parameters are well within the range of earlier FPOP experiments [30, 34, 36, 37, 39, 40, 53]. The width of the laser beam at the irradiation spot was 1 mm, as determined from paper burn patterns; 160 μL capillary outflow aliquots were collected 1 s after labeling in microcentrifuge tubes containing 80 μL of 100 mM phosphate buffer, 5 μM Met, and 1 μM catalase prior to flash freezing in liquid nitrogen and lyophilization. Background oxidation is negligible under these conditions (Supporting Figure S1). Intact protein mass analyses were performed on a Synapt G2 ESI mass spectrometer (Waters, Milford, MA, USA) that was coupled to a Waters UPLC employing a 1.7 μm C4 (BEH300) 2.1 mm × 50 mm reversed-phase column. A detailed analysis of apo-Mb oxidation patterns by MS/MS-based peptide mapping has been reported previously [35]. For this reason, the current work only focuses on intact protein spectra.

Flash Photolysis

Ideally, one would monitor the temporal evolution of reactive species in situ (i.e., directly within the FPOP continuous-flow system). Unfortunately, the small dimensions and the unfavorable geometry of the capillary setup complicate such endeavors. For optical measurements, the FPOP capillary was therefore replaced with a 3 cm^3 quartz cuvette that was centered in the beam of the excimer laser. A shutter was used to provide single-shot conditions. All other conditions were as described above. The cuvette was emptied and refilled with fresh solution after each excimer laser shot. Time-dependent chemical changes triggered by the 248 nm pulse were probed in orthogonal geometry using a continuous-wave diode-pumped solid-state laser (200 mW at either 532 nm or 635 nm) powered by an U8031A voltage supply (Agilent, Santa Clara, CA, USA). Cut-off filters were used to eliminate spurious infrared emission, and dry ice cooling was used to stabilize the probe laser output. After passing through the sample, the probe laser intensity was recorded using a fast photodiode (FDS100; Thorlabs, Newton, NJ, USA). The output of this detector was connected to a DC9240 digital oscilloscope (Yokogawa, Tokyo, Japan), and the signal was sampled with a resolution of 16 ns per data point. Owing to memory limitations, only 2 × 625,000 contiguous points could be recorded, for a total of 2 × 10 ms. These two windows were adjusted to cover the initial reaction kinetics starting at $t = -2$ ms, as well as the time range around 1 s. A schematic depiction of the flash photolysis setup is provided in Supporting Figure S2.

Excimer-laser induced photochemistry induces bleaching of the reporter dye, which causes the light intensity J monitored by the photodiode to increase. Time-dependent signals recorded in this way are displayed as absorbance difference ΔA, calculated as

$$\Delta A(t) = \log\frac{J_0}{J(t)} \quad (3)$$

where J_0 is the light intensity averaged over 2 ms preceding the 248 nm laser pulse event, and $J(t)$ is the light intensity after the excimer pulse.

Results and Discussion

Choice of Reporter Dye

For characterizing kinetic processes in the FPOP solution we monitored the bleaching of a reporter dye by flash photolysis. A key criterion for choosing a suitable chromophore is the presence of an absorption band in the visible range that can be probed with a standard continuous-wave laser. This excludes some dyes that had been used earlier for FPOP dosimetry [52]. Initial experiments for the current work employed rhodamine 6G, which can be probed at 532 nm. A potential problem with this chromophore is the overlap of the 248 nm excimer laser with a strong absorption band (Supporting Figure S3a). This situation may cause unexpected photochemistry. Cyanine-5 azide (Cy5) has a lower absorption intensity at 248 nm, and it shows less $^1O_2$-induced photobleaching (discussed below). We thus chose Cy5 as reporter dye for all subsequent experiments. Chemical transformations were

probed at 635 nm (Supporting Figure S3b). The use of Cy5 and related compounds for radical dosimetry in biological samples is well established [54–56]. Cy5 possesses amide and aliphatic functionalities, in addition to two indole-like moieties that resemble Trp side chains (Supporting Figure S4a). Hence, it is reasonable to assume that conditions resulting in Cy5 degradation would also result in protein modifications. This view is in line with the use of non-proteinaceous dosimeter dyes in many previous protein ·OH labeling studies [21, 25, 52]. Cy5 concentrations were kept low (5 μM) to minimize interferences with the radical chemistry of the sample (see SI for additional details).

Reporter Dye Background Reactivity

Prior to exposing Cy5 to FPOP conditions, it is important to characterize its background reactivity. We thus first conducted experiments in the absence of H_2O_2, scavenger, or protein. Under these conditions, the 248 nm laser pulse causes a ~20 ns wide negative ΔA spike at $t = 0$ (Figure 2a). This signal reflects depletion of the Cy5 ground state and subsequent relaxation of the excited molecule by fluorescence. Following this spike, Cy5 exhibits residual bleaching ($\Delta A \approx -0.03$) that largely recovers within ~5 ms (Figure 2b), consistent with triplet-singlet relaxation [57]. A minor absorbance difference ($\Delta A \approx -0.006$) remains after 1 s, which indicates a low level of irreversible photochemical damage. Permanent photobleaching of organic dyes under the conditions used here is caused by singlet oxygen ($^1O_2$), generated via interaction of dissolved $^3O_2$ with triplet excited states [57–60].

The data of Figure 2 indicate that optical signals observed in FPOP solutions will be somewhat affected by the inherent photophysics and photochemistry of the reporter dye. In particular, near-instantaneous bleaching of $\Delta A \approx -0.03$ reflects triplet formation, rather than oxidation. $^1O_2$-mediated effects are of little concern because the ΔA values seen during FPOP (discussed below) are significantly larger than the long-term effects in Figure 2.

Addition of H_2O_2

We next explored the behavior of Cy5 solutions containing 0.1% H_2O_2, without scavenger or protein. The 248 nm laser pulse results in a maximum signal amplitude of $\Delta A \approx -0.11$ (Figure 3a). This bleaching takes place in two stages. $\Delta A \approx -0.03$ is reached within a few ns, reflecting triplet formation as in Figure 2. The subsequent transition down to $\Delta A \approx -0.11$ occurs over 2 μs. We attribute this second stage to ·OH-mediated oxidation of Cy5, a view that is supported by ESI-MS analysis of the dye solution (Supporting Figure S4). The μs time scale of the Cy5 bleaching kinetics in the presence of H_2O_2 is roughly consistent with the expected ·OH recombination profile of Figure 1a [30]. Disregarding minor triplet relaxation on the ms time scale, ΔA remains stable to the end of the experimental time window at $t \approx 1$ s (Figure 3b), implying that no further chemical changes take place.

Addition of Scavengers

A key aspect of FPOP is the use of scavengers for tuning the ·OH lifetime. The goal of the current study is to explore the solution chemistry under typical FPOP conditions, and hence we primarily focus on Gln, which represents the most widely used scavenger [30–32]. As a next step of our investigation, we thus studied the behavior of Cy5 in 0.1% H_2O_2 and 20 mM Gln (without protein). Exposure to the 248 nm pulsed laser is followed by an unexpectedly slow response. Following a small instantaneous change ($\Delta A \approx -0.03$ due to triplet formation), the absorbance remains constant for more than 10 μs (Figure 3c). Additional bleaching takes place on the time scale of tens of *milli*seconds, culminating in $\Delta A = -0.075$ after 1 s (Figure 3d). Comparable effects were observed for amino acid scavengers other than Gln (Supporting Figure S5). Gln experiments were also repeated at a lower H_2O_2 concentration of 0.01%, resulting in very similar slow bleaching kinetics, albeit with reduced ΔA (data not shown).

Why does Gln slow down Cy5 oxidation in such a dramatic fashion? Without Gln there are few reactions that compete with direct ·OH-mediated oxidation of the reporter dye, causing significant Cy5 degradation during the ·OH lifetime of a few μs (Figure 2a). The presence of 4000-fold excess Gln provides new reaction pathways that compete with ·OH-mediated oxidation of Cy5. Such conditions likely favor the formation of secondary radicals such as Gln-O-O·, and other metastable species (reactions 1 and 2) [46, 47, 49]. The data of Figure 3c

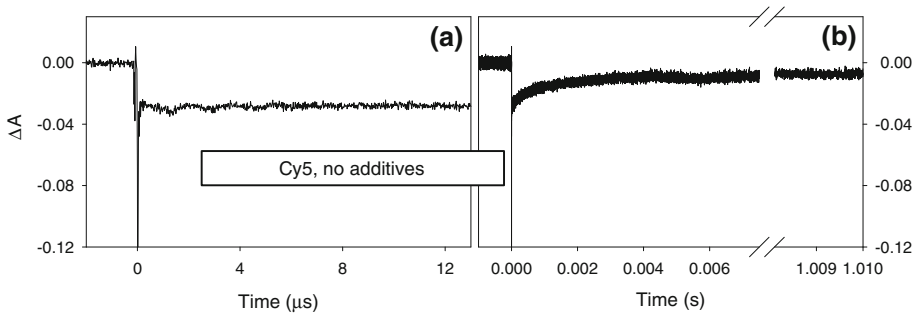

Figure 2. Absorbance changes of the reporter dye Cy5 monitored at 635 nm, following a 248 nm excimer laser pulse at $t = 0$. **(a)** Microsecond range. **(b)** Millisecond to second range. The data were acquired in 10 mM aqueous phosphate buffer (pH 7) without any other additives

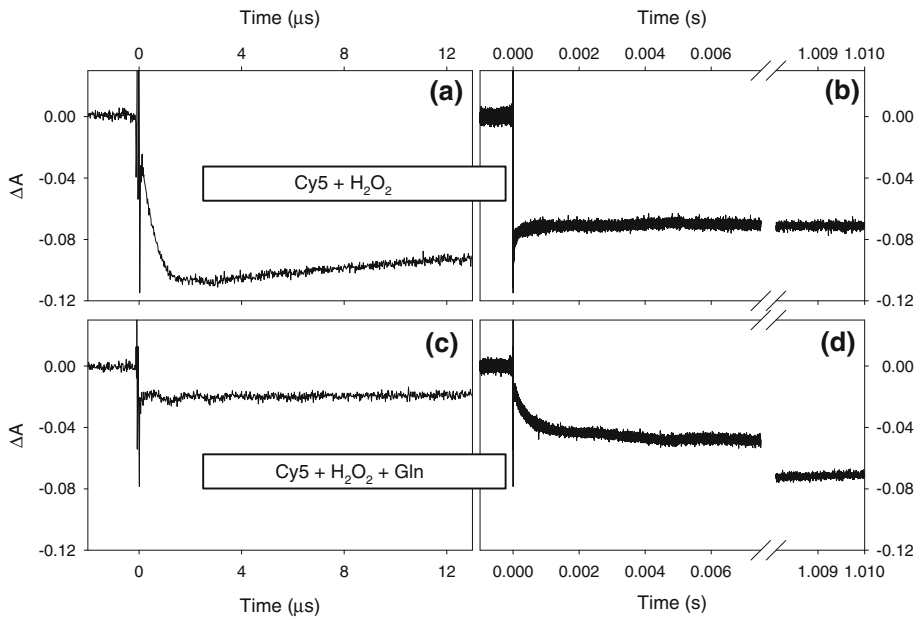

Figure 3. Cy5 absorbance changes triggered by a 248 nm laser pulse at pH 7. **(a)**, **(b)** Phosphate buffer with 0.1% H_2O_2, no scavenger. **(c)**, **(d)** Typical FPOP conditions: 0.1% H_2O_2 and 20 mM Gln

and d indicate that these secondary radicals persist over tens of ms, and that they cause Cy5 oxidation long after ·OH has disappeared from the solution.

In summary, addition of Gln as scavenger dramatically slows down oxidative bleaching of the reporter dye. Instead of shortening the labeling pulse, Gln extends the time scale of Cy5 oxidation by favoring the formation of metastable secondary radicals. Other amino acids are more effective scavengers (e.g., Met at pH 7, Supporting Figure S5). However, scavengers with very high potency are unsuitable for FPOP because they shut down oxidation of the reporter dye (Supporting Figure S5a) and the protein [30].

Flash Photolysis of Protein-Containing Samples

Next we examined the behavior of solutions containing all ingredients typically encountered during FPOP, i.e., H_2O_2, Gln, and protein, in addition to Cy5. Apo-Mb was chosen as model system because it has been extensively studied in earlier FPOP experiments [30, 35]. Measurements were conducted at different pH to explore possible conformational effects. At pH 7, apo-Mb adopts a compact structure, while pH 2 induces large-scale unfolding [61].

Figure 4a and b depict theoretical Cy5 bleaching curves, calculated by assuming that (i) the ·OH concentration follows the "blue" profile of Figure 1b and (ii) that ·OH is the only species causing analyte oxidation. Both points are key paradigms of the FPOP literature [30–32]. For the theoretical curves in Figure 4a and b, maximum bleaching is attained within 1 µs.

Experimental Cy5 profiles acquired at pH 7 show a small absorbance change due to triplet formation at $t \approx 0$. Subsequent large-scale bleaching of the reporter dye extends over at least ~10 ms (Figure 4c, d). Similar data were observed at pH 2 (Figure 4e, f). The kinetics of these protein solutions are not too different from those seen in the absence of apo-Mb (Figure 3c, d). The experimental results of Figure 4 are in stark contrast to the corresponding theoretical FPOP profiles. Cy5 bleaching occurs over ~10^{-2} s rather than 10^{-6} s.

The reporter dye serves as a proxy for solvent-accessible side chains, akin to a dosimeter molecule [21, 25, 52]. We recognize that the intrinsic chemistry of Cy5 is somewhat different from that of amino acid residues. Considering the high reactivity of typical radical compounds, however, it is reasonable to expect that conditions resulting in Cy5 oxidation will also lead to protein oxidation [47, 49]. In other words, our Cy5 bleaching data strongly suggest that protein oxidative labeling during FPOP takes place ~10,000 times more slowly than originally suggested [30–32]. These slow oxidation kinetics are attributed to the presence of metastable secondary radicals, as outlined above.

FPOP Mass Spectra

Irregularities consistent with the results of the preceding sections are evident even in standard FPOP/MS experiments. For illustrating these issues, it is helpful to recall a few basic points. Assuming a homogeneous flow profile [62], the laser frequency f in FPOP is adjusted such that labeled solution segments are separated by regions that do not undergo irradiation [30, 31]. For a laser beam diameter s and flow velocity v the excluded volume fraction [31] is $EVF = 1 - (s \times f)/v$ [62]. Oxidation levels are reported as unmodified fraction, $F_U = I_U / I_{tot}$ where I_U is the ion count of the unoxidized protein, and I_{tot} is the total ion count [25]. Geometric considerations imply that F_U should never be lower than EVF [30, 31]. Hence, experimental data with $F_U << EVF$ indicate the presence of unexpected artifacts.

FPOP of native apo-Mb produced the mass distribution of Figure 5a. These data closely resemble previously published

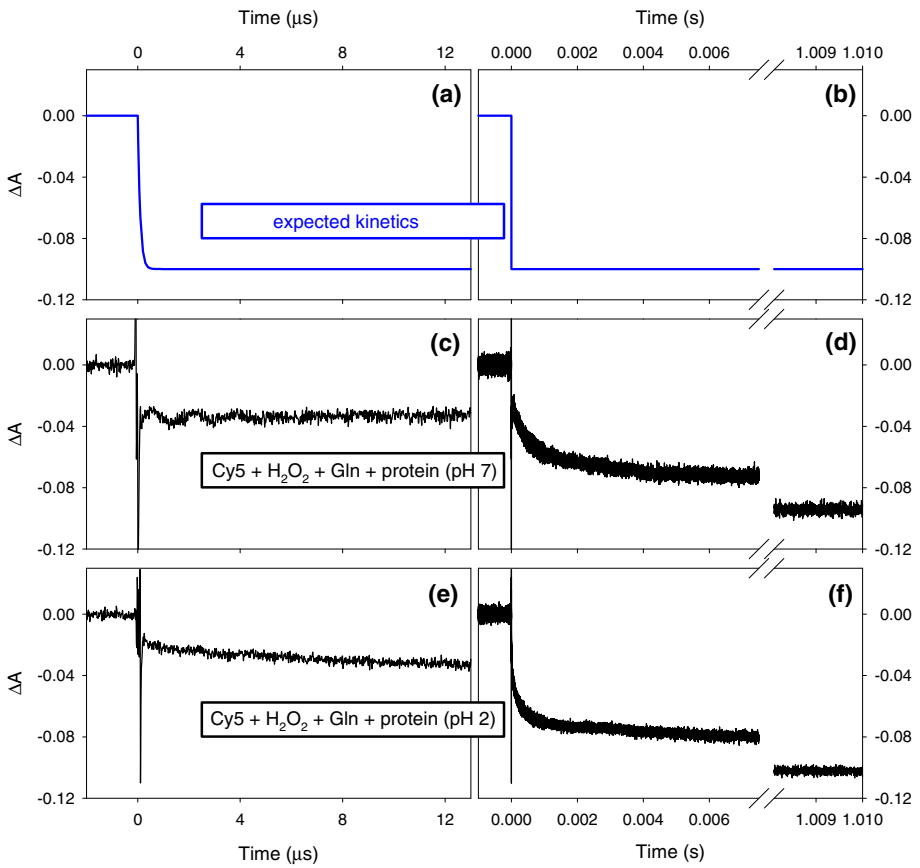

Figure 4. Cy5 absorbance changes under FPOP conditions, with 0.1% H_2O_2, 20 mM Gln, and 10 µM apo-Mb. **(a)**, **(b)** Expected profiles according to reference [30], calculated as described in the Supplementary Information. **(c)**, **(d)** Experimental data acquired at pH 7. **(e)**, **(f)** Experimental data acquired at pH 2

spectra [30], demonstrating that our FPOP conditions are consistent with those used by others. The mass distribution of Figure 5a yields $F_U = 0.21$, in reasonable agreement with the expected value of $EVF = 25\%$. Such comparisons have been used in the past to support the view that FPOP data are consistent with expectations, and that labeling is tightly controllable via a judicious choice of s, f, and v [30, 31]. Surprisingly, there is a dramatic F_U versus EVF mismatch when FPOP is applied to non-native proteins. FPOP of acid-unfolded apo-Mb produces $F_U = 4.3\%$, much lower than the expected value of 25% (Figure 5b). Similarly, FPOP of semi-unfolded barstar with $EVF = 25\%$ [63] resulted in $F_U = 7\%$ (Figure 2a in reference [41]). It is concluded that F_U values in FPOP tend to be too low (i.e., the percentage of oxidized protein is higher than expected). It seems likely that such $F_U \ll EVF$ scenarios arise due to mixing within the capillary after excimer laser exposure, as excluded volume portions come in contact with irradiated flow segments that contain secondary radicals.

Inconsistencies between EVF and F_U have received little attention in the past. Perhaps this is because earlier FPOP work largely focused on native proteins where many side chains are protected by burial, such that overoxidation artifacts are difficult to recognize. Unfolded proteins (as in Figure 5b and reference [41]) are more conducive to stringent F_U versus EVF tests because of their greatly elevated reactivity.

FPOP Without Scavenger

As discussed above, the presence of free Gln extends the FPOP labeling pulse rather than shorten it. This suggests that measurements without scavengers could represent an interesting alternative, although such conditions can induce overoxidation [30]. Cy5 absorption measurements on solutions containing 10 µM native apo-Mb and 0.1% H_2O_2 (without Gln) show that 80% of the total bleaching takes place within 100 µs (Figure 6a, b). This is considerably faster than in the presence of Gln (Figure 4c, d). Nonetheless, bleaching is slower than the µs kinetics seen for solutions containing only Cy5 and H_2O_2 (Figure 3a, b), suggesting that the protein itself can become a reservoir for secondary radicals.

A complication encountered for scavenger-free solutions is the fact that the extent of Cy5 bleaching depends on the protein structure. For acid-unfolded apo-Mb (Figure 6c, d) the total signal amplitude is roughly twice that seen at pH 7 (Figure 6a, b). This observation demonstrates that for scavenger-free samples, the concentration of solvent-accessible side chains affects the radical milieu in the solution. Ten µM apo-Mb is roughly equivalent to the organic content of $(n \times 10)$ µM scavenger, where n is the number of solvent-accessible side chains. For fully unfolded apo-Mb ($n = 153$), this corresponds to an effective amino acid concentration of 1.53 mM. Native apo-Mb is

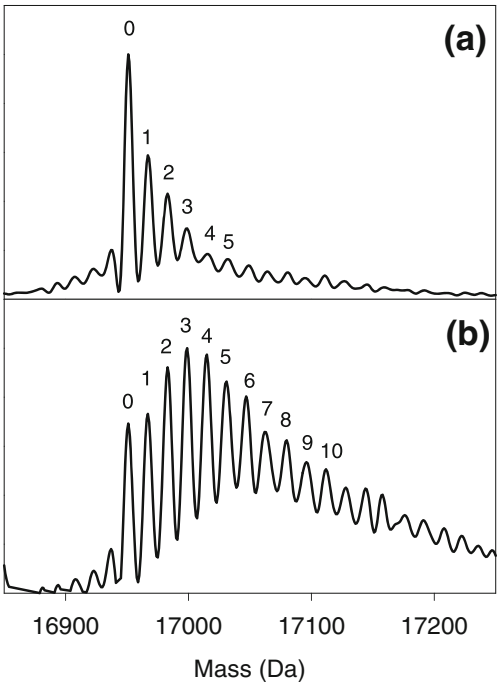

Figure 5. Deconvoluted apo-Mb mass distributions after FPOP in 0.1% H_2O_2 with 20 mM Gln. **(a)** Native protein at pH 7. **(b)** Unfolded protein at pH 2. "0" denotes unmodified apo-Mb, whereas "1", "2", … indicate the number of incorporated oxygens (+16 Da adducts)

characterized by a much lower number of *n*. Hence, in scavenger-free solutions the protein conformation can modulate the behavior of reactive species. In the presence of scavenger (e.g., 20 mM Gln, Figure 4c–f) there is a sufficiently large background concentration of organic moieties that protein unfolding effects become negligible for the Cy5 bleaching kinetics. Hence, scavengers provide improved labeling control in protein conformational studies, but they slow down the oxidation kinetics.

Conclusions

The current work represents the first attempt to characterize the FPOP time scale by applying time-resolved measurements. We find that reporter dye bleaching is four orders of magnitude slower than the 1 μs time scale expected from the FPOP literature [30–32]. Fast (μs) Cy5 bleaching is observed only in the absence of other organic species. The addition of scavengers (such as Gln) or other organic moieties (such as protein) dramatically slows down Cy5 bleaching by favoring the formation of metastable secondary radicals. The discrepancy of expected versus measured time scales uncovered here may be rooted in the misconception that FPOP oxidation is mediated only by direct ·OH/analyte interactions. The wider literature suggests that FPOP conditions will favor the formation of various secondary radicals, and that these species can cause oxidation long after ·OH has disappeared [25, 46, 47, 49]. The reactivity of secondary radicals is lower than that of ·OH, but due to their extended lifetimes they can nonetheless cause significant analyte oxidation [47, 51].

The key question is to what extent the measured Cy5 bleaching profiles reflect the protein oxidation kinetics in FPOP. Side chain oxidation is "UV-Vis silent", such that in situ kinetic experiments are difficult. The use of a non-proteinaceous reporter dye is a way to sidestep this problem, analogous to dosimetry experiments conducted previously by others [21, 25, 52]. The idea underlying those dosimetry

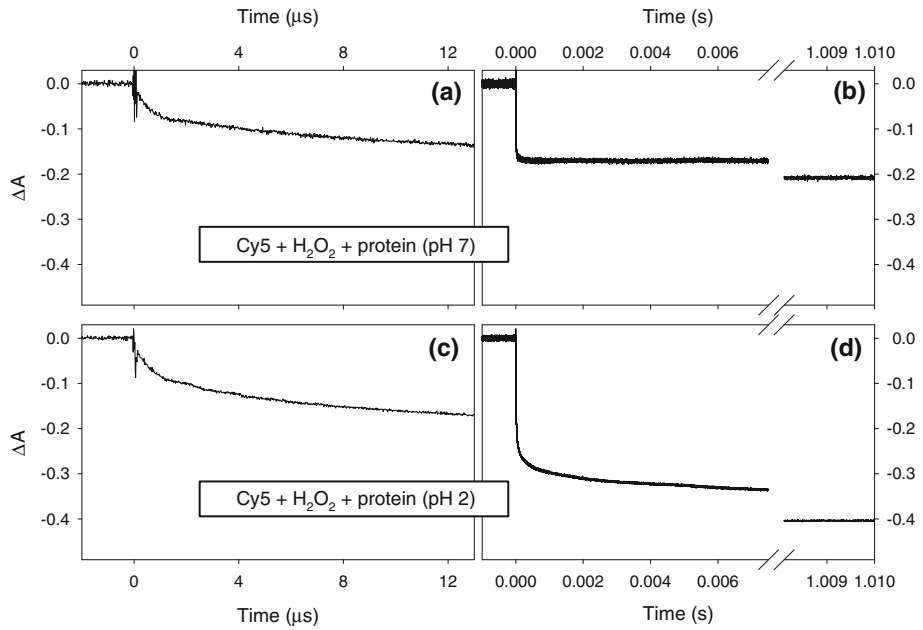

Figure 6. Cy5 absorbance changes under FPOP conditions as in Figure 4, but without scavengers (the solutions contained 0.1% H_2O_2 and 10 μM protein). Data were acquired at pH 7 **(a)**, **(b)** and pH 2 **(c)**, **(d)**. The ΔA scale covers a wider range than in the preceding figures

studies is that the chemical nature of the reporter dye is of secondary importance, keeping in mind that ·OH and many other radicals react indiscriminately with a wide range of organic compounds [25, 46, 47, 49]. The successful use of cyanines for earlier dosimetry applications [54–56] suggests that these considerations also hold for Cy5. Hence, it is likely that the Cy5 bleaching profiles seen in our experiments approximately mirror the time course of protein oxidative labeling during FPOP.

In conclusion, our data suggest that protein oxidative modifications during FPOP are formed within tens of milliseconds (i.e., four orders of magnitude slower than the originally suggested time scale of 1 μs) [30–32]. Sulfur-containing and aromatic side chains will be particularly vulnerable to secondary oxidation because of their high reactivities [25]. Thus, FPOP may not represent a "magic bullet" that is immune to labeling-induced structural artifacts by virtue of ultra-rapid chemistry. Also, the structural information obtainable in submillisecond FPOP folding experiments may be limited [33]. The prospects are more favorable for structural studies on longer time scales and under equilibrium conditions. The possible implications of secondary radicals for pulsed oxidative labeling techniques other than FPOP remain to be investigated.

The issue of secondary oxidation artifacts in protein structural studies has been discussed previously, with focus on much longer time scales (seconds to hours) [64, 65]. For example, it is common practice to mix the FPOP capillary outflow with methionine and catalase for suppressing oxidation mediated by H_2O_2 and other reactive species [30, 35]. In contrast to those earlier studies, the current work focuses on events taking place within tens of milliseconds. Addressing secondary oxidation on the millisecond time scale is challenging because the solution has not yet emerged from the FPOP capillary under typical operating conditions, complicating the addition of solution supplements. It is hoped that future refinements employing novel fluidic approaches, modified solvent additives, and different ways of radical generation will help overcome existing limitations. The spectroscopic technique introduced here provides a tool for benchmarking such future improvements.

Acknowledgments

This work would not have been possible without the expert technical assistance provided by Jon Aukema and John Vanstone. Professor Mark S. Workentin is acknowledged for insightful discussions. The authors thank Victor Yin for critical reading of the manuscript. Funding was provided by the Natural Sciences and Engineering Research Council of Canada.

References

1. Kaltashov, I.A., Bobst, C.E., Abzalimov, R.R.: Mass spectrometry-based methods to study protein architecture and dynamics. Protein Sci. **22**, 530–544 (2013)
2. Heck, A.J.R.: Native mass spectrometry: a bridge between interactomics and structural biology. Nat. Methods **5**, 927–933 (2008)
3. Mehmood, S., Allison, T.M., Robinson, C.V.: Mass Spectrometry of protein complexes: from origins to applications. Annu. Rev. Phys. Chem. **66**, 453–474 (2015)
4. Ashcroft, A.E.: Mass spectrometry and the amyloid problem—how far can we go in the gas phase? J. Am. Soc. Mass Spectrom. **21**, 1087–1096 (2010)
5. Pirrone, G.F., Iacob, R.E., Engen, J.R.: Applications of hydrogen/deuterium exchange MS from 2012 to 2014. Anal. Chem. **87**, 99–118 (2015)
6. Rand, K.D., Zehl, M., Jorgensen, T.J.D.: Measuring the hydrogen/deuterium exchange of proteins at high spatial resolution by mass spectrometry: overcoming gas-phase hydrogen/deuterium scrambling. Acc. Chem. Res. **47**, 3018–3027 (2014)
7. Percy, A.J., Rey, M., Burns, K.M., Schriemer, D.C.: Probing protein interactions with hydrogen/deuterium exchange and mass spectrometry. Anal. Chim. Acta **721**, 7–21 (2012)
8. Marciano, D.P., Dharmarajan, V., Griffin, P.R.: HDX-MS guided drug discovery: small molecules and biopharmaceuticals. Curr. Opin. Struct. Biol. **28**, 105–111 (2014)
9. Leitner, A., Walzthoeni, T., Aebersold, R.: Lysine-specific chemical cross-linking of protein complexes and identification of cross-linking sites using LC-MS/MS and the xQuest/xProphet software pipeline. Nat. Protoc. **9**, 120–137 (2014)
10. Sinz, A., Arlt, C., Chorev, D., Sharon, M.: Chemical cross-linking and native mass spectrometry: a fruitful combination for structural biology. Protein Sci. **24**, 1193–1209 (2015)
11. Fischer, L., Chen, Z.A., Rappsilber, J.: Quantitative cross-linking/mass spectrometry using isotope-labeled cross-linkers. J. Proteomics **88**, 120–128 (2013)
12. Bruce, J.E.: In vivo protein complex topologies: sights through a cross-linking lens. Proteomics **12**, 1565–1575 (2012)
13. Serpa, J.J., Patterson, A.P., Pan, J.X., Han, J., Wishart, D.S., Petrotchenko, E.V., Borchers, C.H.: Using multiple structural proteomics approaches for the characterization of prion proteins. J. Proteomics **81**, 31–42 (2013)
14. Mendoza, V.L., Vachet, R.W.: Probing protein structure by amino acid-specific covalent labeling and mass spectrometry. Mass Spectrom. Rev. **28**, 785–815 (2009)
15. Kahsai, A.W., Rajagopal, S., Sun, J.P., Xiao, K.H.: Monitoring protein conformational changes and dynamics using stable-isotope labeling and mass spectrometry. Nat. Protoc. **9**, 1301–1319 (2014)
16. Collier, T.S., Diraviyam, K., Monsey, J., Shen, W., Sept, D., Bose, R.: Carboxyl group footprinting mass spectrometry and molecular dynamics identify key interactions in the HER2-HER3 receptor tyrosine kinase interface. J. Biol. Chem. **288**, 25254–25264 (2013)
17. Chen, S.-H., Russell, W.K., Russell, D.H.: Combining chemical labeling, bottom-up and top-down ion-mobility mass spectrometry to identify metal-binding sites of partially metalated metallothionein. Anal. Chem. **85**, 229–3237 (2013)
18. Jumper, C.C., Bomgarden, R., Rogers, J., Etienne, C., Schriemer, D.C.: High-resolution mapping of carbene-based protein footprints. Anal. Chem. **84**, 441–4418 (2012)
19. Geer, M.A., Fitzgerald, M.C.: Characterization of the *Saccharomyces cerevisiae* ATP-interactome using the iTRAQ-SPROX tTechnique. J. Am. Soc. Mass Spectrom. **27**, 233–243 (2016)
20. Bridgewater, J.D., Lim, J., Vachet, R.W.: Transition metal-peptide binding studied by metal-catalyzed oxidation reactions and mass spectrometry. Anal. Chem. **78**, 2432–2438 (2006)
21. Shcherbakova, I., Mitra, S., Beer, R.H., Brenowitz, M.: Fast Fenton footprinting: a laboratory-based method for the time-resolved analysis of DNA, RNA and proteins. Nucleic Acids Res. **34**, e48 (2006)
22. McClintock, C.S., Hettich, R.L.: Experimental approach to controllably vary protein oxidation while minimizing electrode adsorption for boron-doped diamond electrochemical surface mapping applications. Anal. Chem. **85**, 213–219 (2013)
23. Maleknia, S.D., Downard, K.: Radical approaches to probe protein structure, folding, and interactions by mass spectrometry. Mass Spectrom. Rev. **20**, 388–401 (2001)
24. Nukuna, B.N., Sun, G., Anderson, V.E.: Hydroxyl radical oxidation of cytochrome *c* by aerobic radiolysis. Free Radic. Biol. Med. **37**, 1203–1213 (2004)
25. Xu, G., Chance, M.R.: Hydroxyl radical-mediated modification of proteins as probes for structural proteomics. Chem. Rev. **107**, 3514–3543 (2007)
26. Watson, C., Janik, I., Zhuang, T., Charvatova, O., Woods, R.J., Sharp, J.S.: Pulsed electron beam water radiolysis for submicrosecond hydroxyl radical protein footprinting. Anal. Chem. **81**, 2496–2505 (2009)

27. Aye, T.T., Low, T.Y., Sze, S.K.: Nanosecond laser-induced photochemical oxidation method for protein surface mapping with mass spectrometry. Anal. Chem. **77**, 5814–5822 (2005)
28. Sharp, J.S., Becker, J.M., Hettich, R.L.: Analysis of protein solvent accessible surfaces by photochemical oxidation and mass spectrometry. Anal. Chem. **76**, 672–683 (2004)
29. Pilau, E.J., Iglesias, A.H., Gozzo, F.C.: A new label-free approach for the determination of reaction rates in oxidative footprinting experiments. Anal. Bioanal. Chem. **405**, 7679–7686 (2013)
30. Hambly, D.M., Gross, M.L.: Laser flash photolysis of hydrogen peroxide to oxidize protein solvent-accessible residues on the microsecond timescale. J. Am. Soc. Mass Spectrom. **16**, 2057–2063 (2005)
31. Gau, B.C., Sharp, J.S., Rempel, D.L., Gross, M.L.: Fast photochemical oxidation of protein footprints faster than protein unfolding. Anal. Chem. **81**, 6563–6571 (2009)
32. Niu, B., Zhang, H., Giblin, D., Rempel, D.L., Gross, M.L.: Dosimetry determines the initial OH radical concentration in fast photochemical oxidation of proteins (FPOP). J. Am. Soc. Mass Spectrom. **26**, 843–846 (2015)
33. Gruebele, M.: Weighing up protein folding. Nature **468**, 640–641 (2010)
34. Li, Z.X., Moniz, H., Wang, S., Ramiah, A., Zhang, F.M., Moremen, K.W., Linhardt, R.J., Sharp, J.S.: High structural resolution hydroxyl radical protein footprinting reveals an extended Robo1-heparin binding interface. J. Biol. Chem. **290**, 10729–10740 (2015)
35. Vahidi, S., Stocks, B.B., Liaghati-Mobarhan, Y., Konermann, L.: Mapping pH-induced protein structural changes under equilibrium conditions by pulsed oxidative labeling and mass spectrometry. Anal. Chem. **84**, 9124–9130 (2012)
36. Farrokhi, V., Bajrami, B., Nemati, R., McShane, A.J., Rueckert, F., Wells, B., Yao, X.D.: Development of structural marker peptides for cystic fibrosis transmembrane conductance regulator in cell plasma membrane by reversed-footprinting mass spectrometry. Anal. Chem. **87**, 8603–8607 (2015)
37. Espino, J.A., Mali, V.S., Jones, L.M.: Cell footprinting coupled with mass spectrometry for the structural analysis of proteins in live cells. Anal. Chem. **87**, 7971–7978 (2015)
38. Poor, T.A., Jones, L.M., Sood, A., Leser, G.P., Plasencia, M.D., Rempel, D.L., Jardetzky, T.S., Woods, R.J., Gross, M.L., Lamb, R.A.: Probing the paramyxovirus fusion (F) protein-refolding event from pre- to postfusion by oxidative footprinting. Proc. Natl. Acad. Sci. U. S. A. **111**, E2596–E2605 (2014)
39. French, K.C., Roan, N.R., Makhatadze, G.I.: Structural characterization of semen coagulum-derived SEMI (86-107) amyloid fibrils that enhance HIV-1 infection. Biochemistry **53**, 3267–3277 (2014)
40. Calabrese, A.N., Ault, J.R., Radford, S.E., Ashcroft, A.E.: Using hydroxyl radical footprinting to explore the free energy landscape of protein folding. Methods **89**, 38–44 (2015)
41. Chen, J., Rempel, D.L., Gross, M.L.: Temperature jump and fast photochemical oxidation probe submillisecond protein folding. J. Am. Chem. Soc. **132**, 15502–15504 (2010)
42. Vahidi, S., Stocks, B.B., Liaghati-Mobarhan, Y., Konermann, L.: Submillisecond protein folding events monitored by rapid mixing and mass spectrometry-based oxidative labeling. Anal. Chem. **85**, 8618–8625 (2013)
43. Wu, L., Lapidus, L.J.: Combining ultrarapid mixing with photochemical oxidation to probe protein folding. Anal. Chem. **85**, 4920–4924 (2013)
44. Liuni, P., Zhu, S.L., Wilson, D.J.: Oxidative protein labeling with analysis by mass spectrometry for the study of structure, folding, and dynamics. Antioxid. Redox Signal. **21**, 497–510 (2014)
45. Heinkel, F., Gsponer, J.: Determination of protein folding intermediate structures consistent with data from oxidative footprinting mass spectrometry. J. Mol. Biol. **428**, 365–371 (2015)
46. Buxton, G.V., Greenstock, C.L., Helman, W.P., Ross, A.B.: Critical review of rate constants for reactions of hydrated electrons, hydrogen atoms and hydroxyl radicals (.OH/.O) in aqueous solution. J. Phys. Chem. Ref. Data **17**, 513–886 (1988)
47. Von Sonntag, C., Schuchmann, H.P.: The elucidation of peroxyl radical reactions in aqueous solution with the help of radiation-chemical methods. Angew. Chem. Int. Ed. Engl. **30**, 1229–1253 (1991)
48. Gau, B.C., Chen, H., Zhang, Y., Gross, M.L.: Sulfate radical anion as a new reagent for fast photochemical oxidation of proteins. Anal. Chem. **82**, 7821–7827 (2010)
49. Neta, P., Grodkowski, J., Ross, A.B.: Rate constants for reactions of aliphatic carbon-centered radicals in aqueous solution. J. Phys. Chem. Ref. Data **25**, 709–1050 (1996)
50. Monig, J., Gobl, M., Asmus, K.D.: Free radical one-electron versus hydroxyl radical-induced oxidation. Reaction of trichloromethylperoxyl radicals with simple and substituted aliphatic sulphides in aqueous solution. J. Chem. Soc. Perkin Trans. **2**, 647–651 (1985)
51. Galano, A., Muñoz-Rugeles, L., Alvarez-Idaboy, J.R., Bao, J.L., Truhlar, D.G.: Hydrogen abstraction reactions from phenolic compounds by peroxyl radicals: multireference character and density functional theory rate constants. J. Phys. Chem. A. (2015). doi:10.1021/acs.jpca.5b07662
52. Xie, B., Sharp, J.S.: Hydroxyl radical dosimetry for high flux hydroxyl radical protein footprinting applications using a simple optical detection method. Anal. Chem. **87**, 10719–10723 (2015)
53. Charvatova, O., Foley, B.L., Bern, M.W., Sharp, J.S., Orlando, R., Woods, R.J.: Quantifying protein interface footprinting by hydroxyl radical oxidation and molecular dynamics simulation: application to galectin-1. J. Am. Soc. Mass Spectrom. **19**, 1692–1705 (2008)
54. Nakagawa, Y., Hori, H., Yamamoto, I., Terada, H.: Characteristic bleaching profiles of cyanine dyes depending on active oxygen species in the controlled Fenton reaction. Biol. Pharm. Bull. **16**, 1061–1064 (1993)
55. Yuan, L., Lin, W.Y., Song, J.Z.: Ratiometric fluorescent detection of intracellular hydroxyl radicals based on a hybrid coumarin-cyanine platform. Chem. Commun. **46**, 7930–7932 (2010)
56. Kundu, K., Knight, S.F., Willett, N., Lee, S., Taylor, W.R., Murthy, N.: Hydrocyanines: a class of fluorescent sensors that can image reactive oxygen species in cell culture, tissue, and in vivo. Angew. Chem. Int. Ed. **48**, 299–303 (2009)
57. Gilbert, A., Baggott, J.: Essentials of Molecular Photochemistry. Blackwell, London (1991)
58. Zheng, Q.S., Jockusch, S., Zhou, Z., Altman, R.B., Warren, J.D., Turro, N.J., Blanchard, S.C.: On the mechanisms of cyanine fluorophore photostabilization. J. Phys. Chem. Lett. **3**, 2200–2203 (2012)
59. Ogilby, P.R.: Singlet oxygen: there is indeed something new under the sun. Chem. Soc. Rev. **39**, 3181–3209 (2010)
60. Schweitzer, C., Schmidt, R.: Physical mechanisms of generation and deactivation of singlet oxygen. Chem. Rev. **103**, 1685–1757 (2003)
61. Eliezer, D., Yao, J., Dyson, H.J., Wright, P.E.: Structural and dynamic characterization of partially folded states of apomyoglobin and implications for protein folding. Nat. Struct. Biol. **5**, 148–155 (1998)
62. Konermann, L., Stocks, B.B., Czarny, T.: Laminar flow effects during laser-induced oxidative labeling for protein structural studies by mass spectrometry. Anal. Chem. **82**, 6667–6674 (2010)
63. Chen, J., Rempel, D.L., Gau, B., Gross, M.L.: Fast photochemical oxidation of proteins and mass spectrometry follow submillisecond protein folding at the amino-acid level. J. Am. Chem. Soc. **134**, 18724–18731 (2012)
64. Xu, G., Kiselar, J., He, Q., Chance, M.R.: Secondary reactions and strategies to improve quantitative protein footprinting. Anal. Chem. **77**, 3029–3037 (2005)
65. Hambly, D.M., Gross, M.L.: Cold chemical oxidation of proteins. Anal. Chem. **81**, 7235–7242 (2009)